A MODEL FOR THE VAWT AERODYNAMIC BRAKES

Farooq Saeed
King Fahd University of Petroleum & Minerals, Dhahran 31261, Saudi Arabia
farooqs@kfupm.edu.sa

Abstract:The paper presents a mathematical model for the analysis of aerodynamic brakes for use in vertical axis wind turbines (VAWT). The governing equations are derived from the principle of angular momentum conservation and can be posed in terms of either angular velocity or angular displacement as a function of time. Since the primary opposing force is the braking torque due to the aerodynamic drag resistance of the brakes, the model can be used to size the brakes in terms of the speed with which the rotor must be brought to rest. A basic limitation of the current model for the aerodynamic brakes is that it does not include the effect of the diminishing torque as a result of slowing down of the rotor.

1.Introduction

The objective of this study is to design the aerodynamic brakes for a typical VAWT depicted in Fig. 1. The aerodynamic brakes act as flow spoilers and can be deployed in a variety of ways to directly counter-act the rotor torque [1, 2]. Although many possible designs and shapes of the spoilers could be employed for the task, Fig. 1 shows four of the more simplest types that are not only easy to incorporate into a VAWT design but also very effective in their resistance to counter the rotor torque. These four simple types are: (1) Sail-type flat rectangular shaped spoilers on rotor tower, (2) Bucket-type semi-circular shaped spoilers on rotor tower, (3) Blade spoilers similar to those used on aircraft wings on rotor blades, and (4) Torque-limiting blade pitch. Figures 2a through 2d shows the above four types in their retracted and deployed configurations.

Since the VAWT tower is fixed, the choice of aerodynamic brake is limited to either having spoilers on the rotor blades (Fig. 2c) or using a torque-limiting blade pitch mechanism (Fig. 2d) to effectively stop the rotor. The choice of the spoiler is dictated by the degree of resistance offered by the configuration which depends on its 2D cross-sectional drag coefficient. Figure 3 shows drag coefficient [3] of several simple 3D and 2D shapes. In Figure 3, shapes (18) through (22) offer some of the highest 2D drag coefficients and amongst these shapes, the flat plate (shape 18) and the angled plate (shape 21) are probably the simplest to use and deploy on the rotor blades.

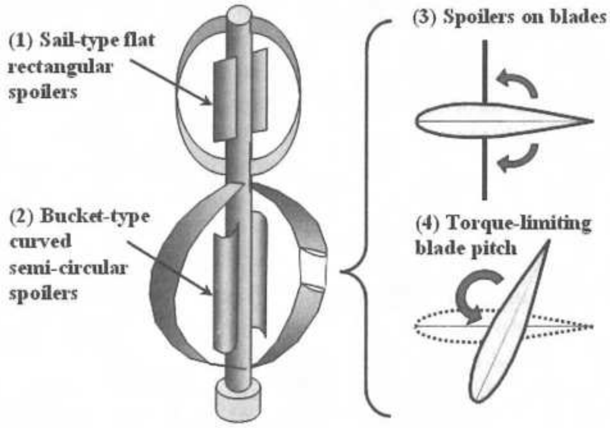

Figure 1: The VAWT aerodynamic brake concept

For the current study, the flat-plate type configuration, shape (18), was chosen since it will be easier to install and deploy on the rotor blade and also since it offers a high drag ($C_D = 1.98$). It is assumed that the straight blade segments of the rotor will incorporate the spoilers. The objective is then to determine the optimum area of the spoilers to effectively slow down the rotor

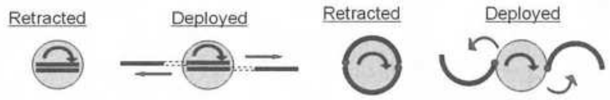

(a) Sail-type on tower. (b) Bucket-type on tower.

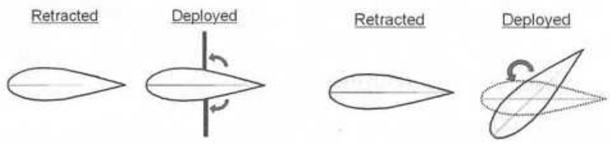

(c) Blade spoilers (d) Torque-limiting blade pitch

Figure 2: Cross-section views of rotor tower and blade shown to depict different types of spoilers and their method of deployment to counter the rotor torque.

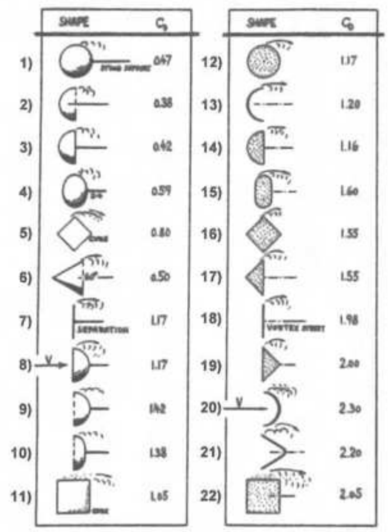

Figure 3: Drag Coefficient of several simple 3D (left) and 2D shapes (right) [3].

2. Methodology

In order to determine the size (area) of the brakes required to counter the rotor torque, the angular momentum/torque conservation principle can be applied which is simply:

Rotor torque + Rotor momentum – Rotor Drag Torque – Braking torque = Net angular momentum

Thus, the above conservation principle yields the following differential equation:

$$\tau_{rotor} + \alpha I - \tau_{drag} - \tau_{brake} = m \frac{d_{\theta}}{d} \qquad (1)$$

where*t*is the torque,*a*is the angular acceleration, I is the moment of inertia of the rotor blades and struts, $c_q$is the tangential velocity of the rotor, m mass of the rotor and struts and an average radius r (rotor mass center). Since the rotor torque has a sinusoidal form, the above equation can also be written as:

$$\begin{aligned}&(\tau_{rotor,\max} - \tau_{rotor,\min})\sin(a\omega t + b)\\&+\alpha I - \frac{1}{2}\rho\left(rSC_D\big|_{brake} + rSC_D\big|_{rotor}\right)c_\theta^2 = mr\frac{dc_\theta}{dt}\end{aligned} \qquad (2)$$

where*a* and b are constants used to approximate the actual rotor torque with a sinusoidal function. Expressing angular acceleration α in terms of angular velocity*w*we get:

$$\begin{aligned}&(\tau_{rotor,\max} - \tau_{rotor,\min})\sin(a\omega t + b)\\&+I\frac{d\omega}{dt} - \frac{1}{2}\rho\left(rSC_D\big|_{brake} + rSC_D\big|_{rotor}\right)c_\theta^2 = mr\frac{dc_\theta}{dt}\end{aligned} \qquad (3)$$

And, replacing angular velocity ω with the tangential velocity c_θ, we get:

$$\begin{aligned}&(\tau_{rotor,\max} - \tau_{rotor,\min})\sin(ac_\theta t / r + b)\\&+\frac{I}{r}\frac{dc_\theta}{dt} - \frac{1}{2}\rho\left(rSC_D\big|_{brake} + rSC_D\big|_{rotor}\right)c_\theta^2 = mr\frac{dc_\theta}{dt}\end{aligned} \qquad (4)$$

Re-arranging yields:

$$\begin{aligned}&(\tau_{rotor,\max} - \tau_{rotor,\min})\sin(ac_\theta t / r + b)\\&-\frac{1}{2}\rho\left(rSC_D\big|_{brake} + rSC_D\big|_{rotor}\right)c_\theta^2 = \left(mr - \frac{I}{r}\right)\frac{dc_\theta}{dt}\end{aligned} \qquad (5)$$

or by replacing the tangential velocity $c_q$with $r\omega$, the above equation can also be written in terms of the angular velocity ω as:

$$\begin{aligned}&(\tau_{rotor,\max} - \tau_{rotor,\min})\sin(a\omega t + b)\\&-\frac{1}{2}\rho\left(r^3SC_D\big|_{brake} + r^3SC_D\big|_{rotor}\right)\omega^2 = \left(mr^2 - I\right)\frac{d\omega}{dt}\end{aligned} \qquad (6)$$

where r_{brake} is moment arm of the brake torque and is equal to the radial distance of the brake from the center of the tower column, S_{brake} is the total projected area (area normal to the torque) of all brakes, $C_{D,brake}$ = 1.98 is the 2D drag coefficient of the flat-plate type brake based on its 2D cross-sectional shape, r_{rotor} is moment arm (based on mass center) of the rotor and struts drag torque, S_{rotor} is the total projected area (area normal to the torque) of rotor and struts, and $C_{D,rotor}$ = 0.01 is the NACA 0018 airfoil 2D drag coefficient.The above differential equations (5) and (6) are solved using an explicit fourth and fifth-order Runge-Kutta scheme known as the Dormand-Prince pair [4]. Since equations (5) and (6) are first-order differential equations, an initial condition is required to solve the equations.

These initial conditions were based on the turbine torque output for the typical 4 MW VAWTfor a wind speed = 25 m/s and a rotational speed = 1.28 rad/s (see Fig. 4). A 4 MW VAWTwith twin rotors depicted in Fig. 1 was selected for this aerodynamic brake sizing study. The blades have a parabolic shape but each blade is made up of 5 straight sections of varying span to allow use of spoilers. Thus, the initial condition for the ordinary differential equation (5) is at $t = 0$, $c_\theta = r_{ave}\omega$, r_{ave} = average rotor radius, ω = 1.28 rad/s or in terms of angular velocity *w*for the ordinary differential equation (6) is at $t = 0$, ω = 1.28 rad/s. With these initial conditions, the differential equations (5) and (6) were solved using the explicit fourth and fifth-order Runge-Kutta scheme in MATLAB. The results of the analysis and design are presented in the next section both in terms of the final tangential velocity or rotational speed achieved based on the size (area) of the selected brake configuration. Finally, the conclusions present the spoiler chord and span sizing results for the rotor angular velocity of 1.28 rad/s case.

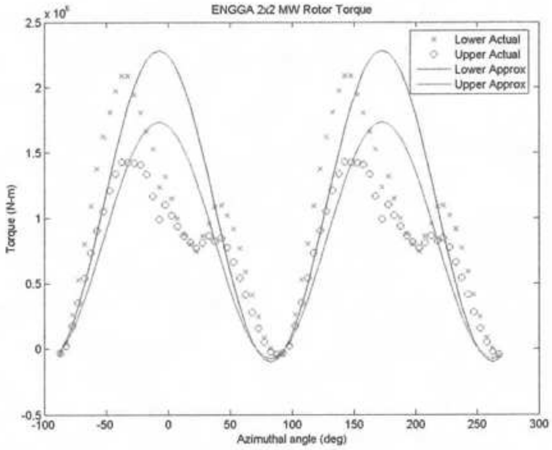

Figure 4: Actual vs. sinusoidal torque.

The analysis was performed in two parts by considering the lower and upper rotors separately. The actual rotor torque was approximated by a sinusoidal function as shown in Fig. 4 to facilitate the solution of the differential equations. A mass per unit length of 70 kg/m was used to estimate the rotor mass as well as the mass center (CG). For the struts, Aluminum was chosen as the material which suggests a single strut mass of 668 kg. The rotor and strut mass calculation results were used to size the aerodynamic brakes for the lower and upper rotors separately. The results are presented in next section.

3. Results and Discussion

3.1 Lower Rotor Brake Sizing

Figure 5 shows the plots of tangential velocity and arc length vs. time obtained from the solution of the differential equation (5) for the lower rotor for optimum span spoilers. Figure 6 shows the plots of and angular velocity and rotation angle vs. time obtained from the solution of the differential equation (6) for the lower rotor for optimum span spoilers. The results show that such optimum span spoilers can effectively slow down the rotor. This is reflected in the tangential and angular velocity plots (solid line in Figs. 5 and 6) where the rotor speed effectively reduces to less than 10% of the initial rotor speed (tangential) of 34.7904 m/s. However, any further reduction in the spoiler area (span or width) is found to be not as effective as optimum span spoiler brakes.

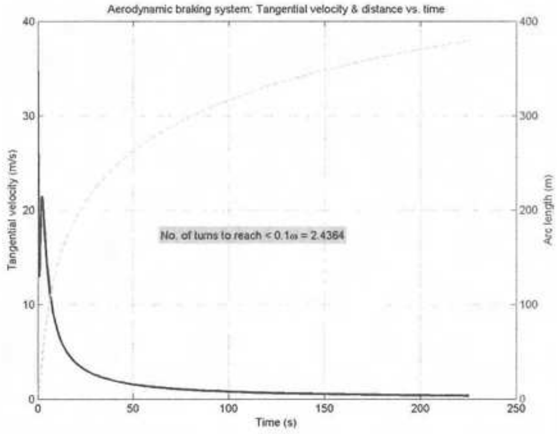

Figure 5: Plot of tangential velocity and arc length vs. time for optimum span spoilers.

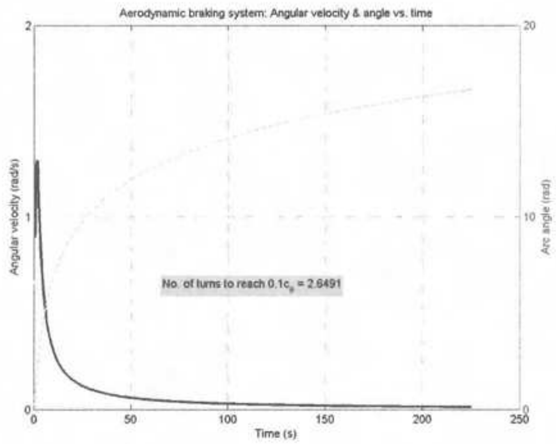

Figure 6: Plot of angular velocity and rotation angle vs. time for optimum span spoilers.

3.2. Upper Rotor Brake Sizing

Figure 7 shows the plots of tangential velocity and arc length vs. time obtained from the solution of the differential equation (5) for the upper rotor for optimum span spoilers. Figure 8 shows the plots of and angular velocity and rotation angle vs. time obtained from the solution of the differential equation (6) for the upper rotor for optimum span spoilers. Similarly, the results show that optimum span spoilers can effectively slow down the rotor. Again, this is reflected in the tangential and angular velocity plots (solid line in Figures) where the rotor speed effectively reduces to less than 10% of the initial rotor speed (tangential) of 32.5504 m/s. However, any further reduction in the spoiler area (span or width) is found to be not as effective as optimum span spoiler brakes. Please note that the dashed line in Figs. 5 through 8 refers to arc length either in meters or radians.

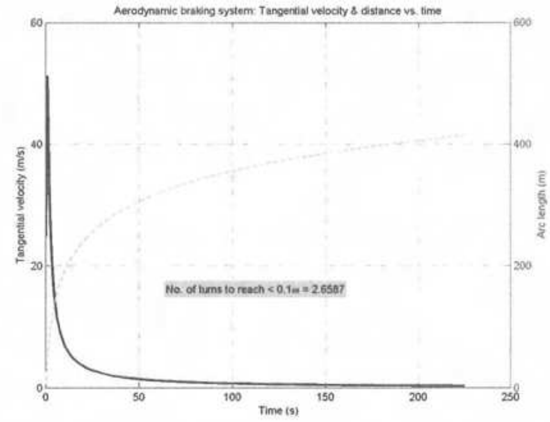

Figure 7: Plot of tangential velocity and arc length vs. time for optimum span spoilers.

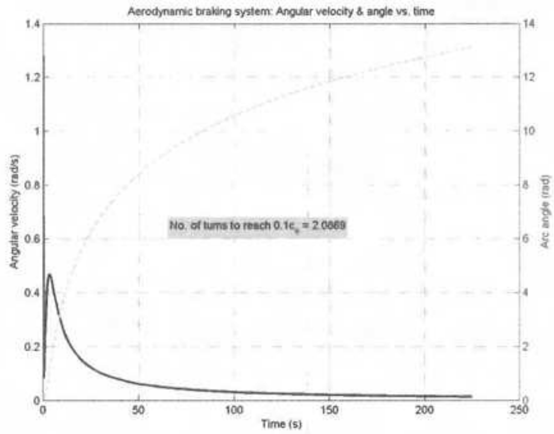

Figure 8: Plot of angular velocity and rotation angle vs. time for optimum span spoilers.

4. Conclusions

The aerodynamic brake sizing study was performed for both lower and upper rotor angular velocity of 1.28 rad/s. The results of the study (optimum span and chord) are shown in Fig. 9 and also listed in Table 1. Note that the total span $b(=b_1+2b_2+2b_3)$ is sum of the spans along the five rotor blade segments where b_1 corresponds to the span of the central segment, b_2 to the two next to central segment and b_3 the two end segments. The resulting size of the spoiler chord c is obtained from the solution of the differential equations discussed earlier. The results also indicate that the total brake area required for the case is approximately 20 m^2 and 16 m^2 for the lower and upper rotors, respectively.

It is noted here that the spoiler span and chord results are based on mass estimates and hence may need revision when exact rotor and strut mass are made available. Moreover, the inertia of the rotors is a major contributor towards the brake sizing. Since the incorporation and deployment of the spoilers in the existing rotor may be challenging, a more convenient or practical method to affect braking would be the use of torque-limiting pitch. This concept is covered under the pitch optimization section of the report.

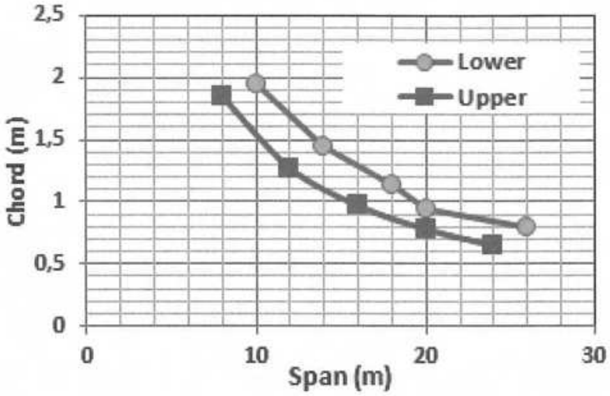

Figure 9: Optimum spoiler span and chord sizing chart forω= 1.28 rad/s.

Table 1: Optimum spoiler span and chord sizing table for ω = 1.28 rad/s.

Lower rotor					
b_1 (m)	b_2 (m)	b_3 (m)	b (m)	c (m)	S (m^2)
10.00	0.00	0.00	10.00	1.95	19.48
10.00	2.00	0.00	14.00	1.44	20.12
10.00	4.00	0.00	18.00	1.14	20.50
10.00	6.00	0.00	20.00	0.94	20.74
10.00	8.00	0.00	26.00	0.80	20.92

Upper rotor					
b_1 (m)	b_2 (m)	b_3 (m)	b (m)	c (m)	S (m^2)
8.00	0.00	0.00	8.00	1.85	14.80
8.00	2.00	0.00	12.00	1.27	15.24
8.00	4.00	0.00	16.00	0.97	15.47
8.00	6.00	0.00	20.00	0.78	15.62
8.00	8.00	0.00	24.00	0.65	15.71

5. References

[1] P. G. Migliore, G. A. Quandt, and L. S. Miller, "Wind Turbine Trailing-Edge Aerodynamic Brakes," Windpower'95, Washington, DC, March 27-30, 1995. NREL/TP-441-7805.

[2] S. Miller, P. G. Migliore, and G. A. Quandt, "An Evaluation of Several Wind Turbine Trailing-Edge Aerodynamic Brakes," J. Sol. Energy Eng. 118(4), 198-203 Nov. 1996.

[3] Drag coefficient [1] of several simple 3D and 2D shapes, web article accessed 30 April 2011at http://aerospaceweb.org/question/aerodynamics/q0231.shtml

[4] Dormand, J. R. and P. J. Prince, "A family of embedded Runge-Kutta formulae," J. Comp. Appl. Math., Vol. 6, 1980, pp 19-26.